

Catalytic behavior of surfactant-containing-MCM-41 mesoporous materials for cycloaddition of 4-nitrophenyl azide

Bouhadjar Boukoussa, Sarah Zeghada, Ghenia Bentabed-Ababsa, Rachida Hamacha, Aïcha Derdour, Abdelkader Bengueddach, Florence Mongin

► **To cite this version:**

Bouhadjar Boukoussa, Sarah Zeghada, Ghenia Bentabed-Ababsa, Rachida Hamacha, Aïcha Derdour, et al.. Catalytic behavior of surfactant-containing-MCM-41 mesoporous materials for cycloaddition of 4-nitrophenyl azide. *Applied Catalysis A: General*, Elsevier, 2015, 489, pp.131-139. 10.1016/j.apcata.2014.10.022 . hal-01096627

HAL Id: hal-01096627

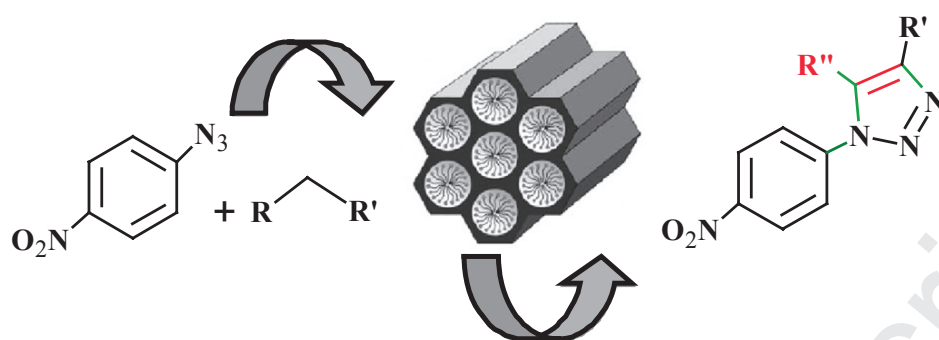
<https://hal-univ-rennes1.archives-ouvertes.fr/hal-01096627>

Submitted on 2 Jul 2015

HAL is a multi-disciplinary open access archive for the deposit and dissemination of scientific research documents, whether they are published or not. The documents may come from teaching and research institutions in France or abroad, or from public or private research centers.

L'archive ouverte pluridisciplinaire **HAL**, est destinée au dépôt et à la diffusion de documents scientifiques de niveau recherche, publiés ou non, émanant des établissements d'enseignement et de recherche français ou étrangers, des laboratoires publics ou privés.

1 Graphical abstract



R	R'	R''
COMe	COMe	Me
COMe	CO_2Me	Me
COMe	CO_2Et	Me
COPh	COPh	Ph
CN	CN	NH_2

2
3

4

5

5 **Highlights**

6

7 ► Synergic effect between homogeneous and heterogeneous catalyst in cycloaddition
8 reactions.

9 ► A facile method for synthesis of triazoles in very short durations (15min).

10 ► Superior catalytic activity and reusability of as-synthesized Si-MCM-41.

11

12

12 Catalytic behavior of surfactant-containing-MCM-41 mesoporous materials

13 For cycloaddition of 4-nitrophenyl azide

14

15 Bouhadjar Boukoussa^a, Sarah Zeghada^b, Ghenia Bentabed Ababsa^b, Rachida Hamacha^{a,*},

16 Aïcha Derdour^b, Abdelkader Bengueddach^a, Florence Mongin^c

17

18 ^a *Laboratoire de Chimie des Matériaux L.C.M, Université d'Oran, BP 1524 El-Mnaouer,*

19 *31000 Oran, Algeria*

20 ^b *Laboratoire de Synthèse Organique Appliquée L.S.O.A, Université d'Oran, BP 1524 El-*

21 *Mnaouer, 31000 Oran, Algeria*

22 ^c *Equipe Chimie et Photonique Moléculaires CPM, Institut des Sciences Chimiques de*

23 *Rennes, UMR 6226, Université de Rennes 1-CNRS, Bâtiment 10A, Case 1003, Campus*

24 *Scientifique de Beaulieu, 35042 Rennes Cedex, France*

25

26 *corresponding author: Rachida Hamacha: hamacha.rachida@univ-oran.dz

27

28

Abstract:

Si-MCM-41, Ga-MCM-41 and Al-MCM-41 mesoporous catalysts (with Si/Al = 80 and Si/Ga= 80) were prepared by direct synthesis under hydrothermal crystallization method using sodium aluminate or gallium sulfate and tetraethyl orthosilicate (TEOS) as aluminum or gallium and silica sources, respectively. The structural features of the materials were determined by various physico-chemical techniques such as X-ray diffraction (XRD), nitrogen sorption at 77 K, Fourier transform infrared spectroscopy (FTIR), scanning and transmission electronic microscopy (SEM, TEM) and thermogravimetric analysis ATG. The catalytic activity of the calcined and as-synthesized catalyst was evaluated through the cycloaddition reaction of 4-nitrophenyl azide with activated alkenes at room temperature under liquid-phase conditions. High yields of 1,2,3-triazole were obtained. For comparison purpose, mixtures of homogeneous and heterogeneous catalyst Et₃N/M-MCM-41 (M=Al or Ga) are also tested. The catalyst was used in five consecutive experiments without important loss of activity, confirming its stability. Finally, a new method for preparing triazoles in short reaction times was developed.

Keywords: mesoporous silica, MCM-41, cycloaddition reaction, triazoles synthesis, surfactant, catalyst re-use.

1. Introduction

The discovery of ordered mesoporous materials M41S by Mobil in 1992 [1] has attracted intense interest due to their large surface areas, well-defined pore structures, inert framework, non toxicity and high biocompatibility [2]. These catalysts are completely recovered after reaction by filtration and are also easily regenerated [3]. The lack of hydrothermal stability of the mesoporous materials has been overcome by the incorporation of heteroatoms such as Al, Ga, Ti, Fe, V, W and Cr [4-7]. These properties allow these mesoporous materials to be used

53 in a wide range of applications such as catalysis [4-7], adsorption [8,10], extraction [11],
54 energy [12], drug delivery systems [13], and for their luminescent character [14].

55 MCM-41 mesoporous materials have drawn the attention of researchers because of their
56 rapid and easy synthesis [15]. Possessing regular pore structure, uniform pore diameter and
57 high surface area [16], they have successfully been employed for typical acid-base or oxido-
58 reduction catalysis such as dehydrogenation of *n*-butane [17], hydrodesulfurization of 4,6-
59 dimethyldibenzothiophene [18], synthesis of benzo[α]xanthenone derivatives [19], oxidation
60 of alcohols and toluene [20], *tert*-butylation of hydroquinone [21], Beckmann rearrangement
61 reaction [22], and cyclohexanone oxime rearrangement [23].

62 Recently several approaches have been proposed to develop basicity in mesoporous
63 materials by dispersing alkali metal oxides in the channel [24,25]. Kloetstra et al. [26] initially
64 proposed to disperse cesium oxide particles in Si-MCM-41 pores. However, due to the
65 treatments used throughout the preparation, its structure was extensively damaged [26].
66 Another way to get basic Si-MCM-41 sites is by functionalizing its surface with organic
67 compounds, particularly with those containing terminal amines in their composition [27,28].
68 These procedures, which are used to generate basic sites on Si-MCM-41, are hard to process
69 and not always lead to the planned basic sites, stable enough for catalysis application. Roy et
70 al [29] have synthesized a new pyridine-imine functionalized mesoporous silica (SBA-15)
71 followed by the grafting of Cu(II) for obtaining a new Cu-PyIm-SBA-15 material and they
72 used these solids like basic catalysts for synthesis of 1,4-disubstituted 1,2,3-triazole.
73 The material is functionalized by anchoring organic bases at the silanol groups, thereby
74 forming a covalent bond. Unfortunately, these organic-inorganic hybrid materials are less
75 basic than the corresponding free organic amine molecule. This fact has been explained as
76 involving the interaction of the amine function with residual silanol groups [30].

77 Mesoporous solids may be used without calcination, the presence of surfactant inside the
78 pores showing interesting and remarkable basic properties. Thus, these attractive catalysts
79 have also been tested in different reactions which require basic catalysts such as Knoevenagel
80 and Claisen–Schmidt condensations [31], Michael additions [32], and cycloaddition reactions
81 of CO₂ with epoxides [33].

82 Kubota et al. [32,34] achieved excellent results during Knoevenagel condensation by using
83 Si-MCM-41 molecular sieve while keeping the surfactant inside the pores called [CTA]Si-
84 MCM-41. In this catalyst, active sites are high basicity SiO⁻ sites, which are in the channels.
85 Oliveira and al [35] used a series of as-synthesized molecular sieves containing several Si/Al
86 ratio and they have been tested as basic catalysts for Knoevenagel condensation, they showed
87 that increasing the content of Si/Al ratio increases the amount of siloxy anion and increases
88 conversion of benzaldehyde.

89 1,2,3-Triazoles have found widespread applications as pharmaceuticals and industrial
90 compounds such as dyes, anticorrosive agents, photostabilizers, photographic materials, and
91 agrochemicals [36]. In addition, compounds containing 1,2,3-triazoles have shown a broad
92 spectrum of biological activities such as antibacterial against Gram positive bacteria [37],
93 herbicidal and fungicidal [38], antiallergic [39], anticonvulsant [40], β -lactamase inhibitive
94 [41] and anti-HIV [42]. Several synthetic methods for preparing triazole derivatives have been
95 developed. Among them, we can cite Huisgen 1,3-dipolar cycloaddition [43] and its recent
96 development towards click chemistry [44].

97 In this paper, we report a facile and rapid pathway for the synthesis of 1,2,3-triazoles
98 through 1,3-dipolar cycloaddition reactions between 4-nitrophenyl azide and activated alkenes
99 [36] using a heterogeneous catalytic system.

100 In previously reported works concerning MCM-41-catalyzed Knoevenagel condensation
101 reactions, as-synthesized Si-MCM-41 was studied as basic catalyst [31-33]. Generally the

102 catalysts for the cycloaddition of azide are solids which contain copper [29,45-47], to our best
103 knowledge, mesoporous Si- Ga or Al-MCM-41 have never been studied for cycloaddition of
104 aryl azides. Thus the aim of the present research is to compare the catalytic properties of a
105 series of mesoporous catalyst including: (1) Si-MCM-41, (2) Ga-MCM-41, (3) Al-MCM-41,
106 (4) and a mixture between homogeneous/heterogeneous catalysts.

107 These mesoporous materials are used as-synthesized or calcined like catalysts for the
108 cycloaddition of aryl azides with activated alkenes in liquid phase at room temperature.

109

110 2. Experimental

111 2.1. Synthesis of Ga-MCM-41 and Al-MCM-41

112 Si-MCM-41, Ga-MCM-41 and Al-MCM-41 mesoporous materials were prepared by
113 direct hydrothermal synthesis using cetyltrimethylammonium bromide (CTAB) as structure-
114 directing template, gallium sulfate or sodium aluminate and TEOS as the gallium or
115 aluminum and silica source, respectively. The procedure for the catalysts preparation was
116 thoroughly described elsewhere [8].

117 The gel composition was: 1 TEOS, 0.12 CTAB, 0.25 NaOH, 1.5 EtOH, 100 H₂O and
118 0.00625 Ga₂(SO₄)₃ (case of Ga-MCM-41) or 0.00625 Al₂O₃ (case of Al-MCM-41) (for the
119 case of Si-MCM-41 the Si/Al or Ga $\approx \infty$). We first prepared two solutions, the first by mixing
120 CTAB (2.91 g, 98%, Alfa Aesar), distilled water (110 mL) and ethanol (6 mL, 99.5%, Riedel-
121 de-Haën) and stirring for 15 min at 308 K, and the second solution by mixing NaOH (0.66 g,
122 98% Sigma-Aldrich), distilled water (10 mL), and the appropriate amount of sodium
123 aluminate (54% Al₂O₃, 41% Na₂O, 5% H₂O, Aldrich) or gallium sulfate (Ga₂(SO₄)₃, 99.99%,
124 Sigma-Aldrich). TEOS (7.4 mL, 98%, Aldrich) and the second solution were added dropwise
125 to the first solution. After ageing at 308 K for 3 h, the obtained mixture was transferred to an
126 autoclave and hydrothermally treated under autogenous pressure at 423 K for 10 h. The

127 obtained product was then removed from the oven and cooled to room temperature. After
128 filtration and washing several times with distilled water, the obtained solid was dried at 333 K
129 for at least 24 h. The powder was then calcined in air at 823 K for 12 h to remove the
130 template.

131 2.2. Characterization

132 The XRD powder diffraction patterns of the Si-MCM-41, Ga-MCM-41 and Al-MCM-41
133 mesoporous materials were obtained with a Bruker AXS D-8 diffractometer using Cu-K α
134 radiation. Nitrogen adsorption was performed at 77 K in a TriStar 3000 V6.04 A volumetric
135 instrument. The samples were outgassed at 353 K prior to the adsorption measurement until a
136 3×10^{-3} Torr static vacuum was reached. The surface area was calculated by the Brunauer–
137 Emmett–Teller (BET) method [48]. The pore size distributions were obtained from the
138 adsorption branch of the isotherm using the Barrett–Joyner–Halenda (BJH) method [49].
139 FTIR spectra of the mesoporous Al, Ga or Si-MCM-41 molecular sieves in the range 400–
140 4000 cm^{-1} were collected on a JASCO (4200) instrument using KBr pellet technique.
141 Thermogravimetric analysis (LABSYS Evo SETARAM) was carried out under air
142 atmosphere in the temperature range 20–800°C with a heating rate of 10°C/min. The energy
143 dispersive X-ray analysis (EDX) jointed to a XL-30 scanning electron microscope was used to
144 calculate the Si/Al and Si/Ga ratios of the aluminum- or gallium-containing MCM-41. The
145 surface topography of the different solids was observed using SEM on a Hitachi 4800S
146 microscope and TEM was performed on a JEOL 1200 EXII device.

147

148 2.3. Reaction procedures for the cycloaddition of 4-nitrophenyl azide with activated alkenes

149 **Procedure 1.** To the required methylene-activated compound (2 mmol) and Et₃N (2
150 mmol) in DMF (2 mL) was added 4-nitrophenyl azide (**1**, 1 mmol), and the mixture was

151 stirred at room temperature for 24 h. The precipitate formed upon addition of H₂O (5 mL) was
152 filtrated, washed with H₂O, dried, and recrystallized from iPrOH.

153 **Procedure 2.** To the required methylene-activated compound (2 mmol) and Et₃N (2
154 mmol) in DMF (2 mL) was added 4-nitrophenyl azide (**1**, 1 mmol) and calcined or as-
155 synthesized mesoporous Si- Ga- or Al-MCM-41 catalyst (10 mol%), and the mixture was
156 stirred at room temperature (TLC monitoring). The precipitate formed upon addition of H₂O
157 (5 mL) was filtrated, washed with H₂O and dried. To remove the catalyst, the precipitate was
158 extracted with acetone. After removal of the solvent, the crude product was recrystallized
159 from iPrOH. Characterization data associated with this article have been previously described
160 [50], except in the case of **3c**.

161 **The characterisation data for the 3c is as fellow Ethyl 5-methyl-1-(4-nitrophenyl)-**
162 **1H-1,2,3-triazole-4-carboxylate (3c).** Yield: 93% (procedure 1). Yellow powder, mp 185
163 °C. ¹H NMR (300 MHz, CDCl₃): 1.45 (t, 3H, H1, *J* = 7.1 Hz), 2.68 (s, 3H, H6), 4.47 (q, 2H,
164 H2, *J* = 7.1 Hz), 7.73 (d, 2H, *J* = 9.1 Hz), 8.46 (d, 2H, *J* = 9.1 Hz). ¹³C NMR (75 MHz,
165 CDCl₃): 10.4 (CH₃), 14.5 (CH₃), 61.5 (CH₂), 125.3 (2 CH), 126.0 (2 CH), 137.6 (C), 139.0
166 (C), 140.4 (C), 148.4 (C), 161.5 (C=O).

167 **Procedure 3.** To the required methylene-activated compound (2 mmol) in DMF (2
168 mL) was added 4-nitrophenyl azide (**1**, 1 mmol) and as-synthesized mesoporous MCM-41
169 catalyst (25 mol%), the mixture was stirred at room temperature (TLC monitoring). The next
170 steps are as above (procedure 2).

171

172 **3. Results and discussion**

173 *3.1. Characterization of the catalysts*

174 The diffraction patterns of the as-synthesized and calcined Si-MCM-41, Ga-MCM-41 and
175 Al-MCM-41 catalysts are given in Fig. 1. The main peaks of the XRD patterns of all the

176 samples are consistent with the characteristic peaks of the hexagonal structure of the MCM-41
177 mesoporous molecular sieves. Si-MCM-41 and Al-MCM-41 exhibits a strong peak
178 respectively at $2\theta = 2.27$ - 2.13 due to (100) reflection lines and three weak signals around
179 3.94 - 3.65 , 4.56 - 4.18 and 6.01 - 5.50 (2θ) corresponding to (110), (200) and (210) reflections,
180 indicating the formation of well-ordered mesoporous materials with hexagonal regularity [51].
181 For Ga-MCM-41 materials, peaks of XRD are broadened as a result of the insertion of
182 amount of Ga. This suggests a more disordered arrangement of channels for the Ga-MCM-41,
183 but keeping a hexagonal structure with good regularity. Similar observations have been shown
184 by Campos et al where they studied the influence of Si/Ga on the structure of MCM-41 [9].
185 The decrease of structure order for Al MCM-41 and particularly for Ga-MCM-41 can be
186 explained by the isomorphous substitution of Ga or Al in MCM-41 framework carried out by
187 a direct synthesis method. [52,53].
188 The unit cell parameter a_0 is calculated from $a_0 = 2d_{100}/\sqrt{3}$, where the d-spacing values are
189 calculated by $n\lambda = 2d \sin\theta$. The observed d spacing and unit cell parameter results (Table 1)
190 are well-matched with the hexagonal $p6mm$ space group.

191 We notice that the calculated cell parameters are 43 , 47 and 48 Å for Si- Al- or Ga-MCM-
192 41 solids, respectively; these results are consistent with the literature, where it has been
193 showed that the incorporation of a heteroatom in the structure of MCM-41 increases the unit
194 cell parameter [9]. This difference is probably due to the bond length of Ga-O, Al-O and Si-
195 O, Ga-O being higher than Al-O and Si-O as consequence of the larger ionic radius of Ga^{3+}
196 than Al^{3+} and Si^{4+} [54]. The change in d-spacing and unit cell parameter compared to siliceous
197 MCM-41 proved the incorporation of gallium or aluminum in the framework.

198 An increase of peak intensity is systematically visible after calcination, assessing more
199 ordered structure after surfactant removal. The (100) reflection becomes sharper and more
200 intense upon calcination, although the (110), (200) and (210) reflections are not well defined

201 and overlap to give a single broad band. A lattice contraction is also observed after calcination
202 due to surfactant removal and to the condensation of silanol (SiOH) groups in the walls.

203 Quantitative data for the estimation of gallium and aluminum incorporation was obtained
204 by EDX analysis. According to the chemical composition used for the synthesis of Ga-MCM-
205 41 and Al-MCM-41, a nominal value of Si/Ga or Si/Al = 80 was expected. However, the
206 Si/Ga and Si/Al ratios, as determined by EDX in the calcined MCM-41, are a little higher,
207 indicating that the amount of heteroatom incorporated in the structure is a little less than the
208 expected one (Table 1). For the same ratios of Si/Ga or Si/Al, the percentage of aluminum in
209 Al-MCM-41 is much more than gallium in Ga-MCM-41. This difference of the gallium
210 content in the starting gel and in the final product has already been revealed by Lin et al
211 (2005) when studying the effect of gallium content in the synthesis of hexagonal silicas. In
212 fact, the yield of Ga in the synthesized solids decreased to around 60% [55].

213 In Table 1, are also given the BET surface area, pore size, wall thickness and pore volume of
214 the calcined Si- Ga- or Al-MCM-41 catalysts. There was a slight increase of the wall
215 thickness in the Ga or Al containing materials, when compared with Si-MCM-41. These
216 results could suggest that there was a modification of the structure, probably due to the
217 introduction of these elements in the framework [56]. Fig. 2 shows the nitrogen adsorption–
218 desorption isotherms of the different solids. All the isotherms are of type IV and exhibit three
219 stages. The first stage is due to monolayer adsorption of nitrogen to the walls of the
220 mesopores at a low relative pressure ($P/P_0 < 0.25$). The second stage is characterized by a
221 steep increase in adsorption ($0.25 < P/P_0 < 0.4$). As the relative pressure increases, the
222 isotherm exhibits a sharp inflection, characteristic of capillary condensation within the
223 uniform mesopores. The third stage ($P/P_0 > 0.4$) in the adsorption isotherm is the gradual
224 increase in volume with P/P_0 , due to multilayer adsorption on the outer surface of the
225 particles. The BJH pore size distribution curves for Si- Al- or Ga-MCM-41 are shown in

226 Fig.S1 (see supporting information). The mesoporous materials Si- or Al-MCM-41 have
227 narrow mesopore size distribution ; in the case of Ga-MCM-41, the BJH pore size distribution
228 further indicates the presence of irregular mesopores. These results are well correlated to the
229 XRD data which already revealed less ordered structure for Ga-MCM-41 solids.

230 It could be seen from Table 1 that the pore diameter of samples increased gradually in the
231 following sequence Si-MCM-41 < Al-MCM-41 < Ga-MCM-41, which suggested generally
232 that heteroatoms incorporation would result in a shift to higher pore size [9].

233 On the other hand, the pore volume and BET surface area decreased basically for Ga-MCM-
234 41. Such decrease in the SSA when gallium was introduced could be partly related to the
235 presence of extra-framework gallium species with lower specific surface area and thus
236 lowering the overall surface area of the final material [57].

237 The FTIR spectra of the calcined and as-synthesized samples are given in Fig.S2 (see
238 supporting information). The presence of absorption bands around 2921 and 2851 cm^{-1} for
239 the as-synthesized materials corresponds to asymmetric and symmetric CH_2 vibrations of the
240 surfactant molecules. The infrared spectrum of the calcined samples indicates a broad envelop
241 around 3500 cm^{-1} , due to O–H stretching of surface hydroxyl groups, bridged hydroxyl
242 groups and adsorbed water molecules, while deformational vibrations of adsorbed molecules
243 cause the adsorption bands at 1626–1638 cm^{-1} . The peaks between 1247 and 1072 cm^{-1} are
244 attributed to the asymmetric stretching of T–O–T (T = Ga or Al). Other groups are observed
245 around 800 and 544 cm^{-1} and the peak at 460 cm^{-1} is due to the bending mode of T–O–T.

246 The thermal properties of the samples were investigated by TGA (Fig. 3). The initial weight
247 loss up to 120 °C is due to desorption of physically adsorbed water. The weight loss from 120
248 to 350 °C is due to organic template. The oxidative desorption of the organic template takes
249 place at 180 °C and the minute quantity of weight loss above 350–550 °C is related to water

250 loss from the condensation of adjacent Si–OH groups to form siloxane bonds. The loss in
251 mass varies according to the following order Si-MCM-41 > Ga-MCM-41 > Al-MCM-41.

252 From the TGA results, one can deduce that the organic template associated with the silanol
253 groups in pure silica MCM-41 can be easily removed at lower temperatures whereas, for the
254 Al-MCM-41 samples, the template has to be removed at higher temperatures due to the
255 stronger interaction of the organic template with the aluminum species.

256 SEM and TEM images of the calcined samples Si- Al- or Ga-MCM-41 are shown in
257 Fig. 4. This information could be required to assess any relationship between catalytic activity
258 and their morphologies. The SEM pictures of the samples are typical of silicate mesoporous
259 materials and show a different morphology with some large elongated agglomerates.
260 Whereas Ga-MCM-41 exhibits particles irregular shape between 0.5-2 μm , Si- or Al-MCM-
261 41 have particle size between 1-2.5 μm .

262 The TEM images show that the Si- or Al-MCM-41 mesoporous catalysts display highly
263 ordered honeycomb-like regular arrangement of hexagonal pores. The TEM pictures of the
264 calcined catalysts are presented in Fig. 4. In the case of Ga-MCM-41, the TEM analysis
265 shows pores of irregular form. These results are in agreement with nitrogen sorption
266 measurements and XRD analysis.

267

268 3.2. Catalytic experiments

269 By reaction of 4-nitrophenyl azide (**1**, 1 equiv.) with the activated alkenes **2** (2 equiv.) in
270 the presence of triethylamine (2 equiv.), and using DMF as the solvent, the 1,2,3-triazoles **3a-**
271 **e** were isolated in moderate to high yields after 24 h reaction time at room temperature (Table
272 2). The reaction proved regioselective. The assignment of the stereochemistry was established
273 by NMR (NOESY, HMBC, and HMQC) and was confirmed by XRD [50].

274 *Cycloaddition reaction using a mixture of homogeneous and heterogeneous*
275 *catalysis.* Table 3 depicts the results using both homogeneous (Et₃N) and heterogeneous
276 (MCM-41) basic catalysts. When compared with triethylamine alone (Table 2), the evaluated
277 mixtures exhibit a very important activity, with very high yields and, except for **3d**, shorter
278 reaction times (0.5 to 2 h, Table 3). In the case of homogenous/heterogeneous catalysis using
279 the calcined or as-synthesized mesoporous materials Si- Ga- or Al-MCM-41, 4-nitrophenyl
280 azide (**1**) was simply added to the activated alkenes **2** (2 equiv.) in the presence of both
281 triethylamine (2 equiv.) and a catalytic amount (10 mol%) of Si- Ga- or Al-MCM-41, using
282 DMF as solvent. The products were collected and washed with water. To remove the catalyst,
283 the precipitate was extracted with acetone, and the solvent was then removed. Good results
284 were obtained under these conditions from 4-nitrophenyl azide (**1**) and all the activated
285 alkenes **2** using Et₃N/calcined mesoporous material Si-MCM-41 (Table 3, entries 21-25). By
286 using Et₃N/calcined Ga- or Al-MCM-41 (Table 3, entries 1-5 and 11-15), Et₃N/as-synthesized
287 Si-MCM-41 (Table 3, entries 26-30) and Et₃N/as-synthesized Ga- or Al-MCM-41 (Table 3,
288 entries 6-10 and 16-20), good yields were still observed using acetylacetone (**2a**), methyl
289 acetoacetate (**2b**) and malonodinitrile (**2e**). However, when using ethyl acetoacetate (**2c**) and
290 α -benzoylacetophenone (**2d**), moderate yields were noted. After recourse to a 24 h contact in
291 the case of **2d**, the product **3d** was purified by column chromatography and isolated in yields
292 ranging from 47 to 84%. The use of the mixtures Et₃N/as-synthesized or calcined Si-MCM-41
293 catalyst led to higher yields than the other catalysts.

294 For the products **3d** and **3e**, if we compare the results obtained using the mixture of basic
295 catalysts (Table 3) with those obtained by homogeneous basic catalysis (Table 2), we can note
296 that the reaction times are reduced and that the yields are always improved using the mixtures
297 of Si- Ga- or Al-MCM-41 (10 mol%) with the Et₃N homogeneous catalyst (2 mmol). These

298 results suggest that the triethylamine is entrapped in the mesoporous materials [57], and acts
299 as a supported catalyst for this reaction.

300 **Cycloaddition reaction using a heterogeneous catalysis.** As-synthesized M-MCM-41
301 (M = Si Ga or Al) materials were also used as base catalysts without adding triethylamine
302 (Fig. 5 and Table 4).

303 - *Effect of the amount of catalyst*

304 In order to understand the influence of the heterogeneous catalysts on the cycloaddition
305 reaction, reactions between 4-nitrophenyl azide (**1**, 1 equiv.) and acetylacetone (**2a**, 1 equiv.)
306 were performed using different amounts of as-synthesized Ga-MCM-41 (Fig. 5). Using 10
307 mol% of as-synthesized Ga-MCM-41 led to a very low 5% yield for 24 h reaction time. This
308 result contrasts with the 90% yield obtained using the same amount of catalyst in the presence
309 of triethylamine for a shorter 1.5 h reaction time (Table 3, entry 6), and suggests a synergic
310 effect between triethylamine and the as-synthesized mesoporous material. One can notice in
311 Fig. 5 that increasing the amount of catalyst has an impact on the reaction yield. Indeed, a 24
312 h reaction time led to a 75% yield using 20 mol% (and 92% yield using 25 mol%) of as-
313 synthesized Ga-MCM-41. The yield obtained after one hour of reaction in the presence of
314 20% of catalyst is low about 7%. Thus, the reaction time can be minimized due to an
315 increased reactivity using both catalysts Et₃N and as-synthesized Ga-MCM-41.

316 - *Cycloaddition reaction using Si- Ga- or Al-MCM-41 catalysts*

317 As expected no products were detectable by using 25 mol% of calcined Si- Ga- or Al-
318 MCM-41 as catalyst for the reaction between 4-nitrophenyl azide (**1**, 1 equiv.) and
319 acetylacetone (**2a**, 1 equiv.) (results not shown). In contrast, very high yields were obtained
320 for the products **3a-c** with a reaction time not more than 0.25 h (15 min) when using 25
321 mol% of as-synthesized Si-MCM-41 (Table 4). The latter is more active than as-synthesized
322 Ga- or Al-MCM-41, Et₃N and the mixed catalyst in these three reactions (results not shown).

323 The basic properties exhibited by as-synthesized Si- Ga- or Al-MCM-41 are due to the
324 presence of siloxy anions ($\equiv\text{SiO}^-$), which exist in combination with the cationic surfactant.
325 Indeed, the existence of the ionic pair ($\equiv\text{SiO}^-$, CTA^+) has been demonstrated by many
326 researchers [35,58,59]. For instance, Oliveira and al studied a variety of as-synthesized
327 molecular sieves and assessed that they have basic sites and can be employed as catalysts for
328 Knoevenagel condensation under mild conditions [35]. Their catalytic activity is mostly
329 dependent on the fraction of silicon framework. Pure siliceous molecular sieves are suggested
330 to contain the highest number of siloxy anions, which are the strong basic sites. The occluded
331 organic cations can interact with the molecular sieves framework, providing the high catalytic
332 activity. Calcined siliceous molecular sieves, which have only silanol groups, show a lower
333 activity. The catalytic activity difference between Si- Ga- or Al-MCM-41 could be caused by
334 a higher concentration of siloxy anions in Si-MCM-41 since it has more silica than Ga- or Al-
335 MCM-41 (see EDX results).

336 Koller et al. [60] have also synthesized MFI zeolites with different amounts of silicon
337 and showed that increasing the content of this element increases the amount of siloxy anion.
338 The same remarks were pointed out by Oliveira et al [35] . Srivastava et al. also noticed
339 similar behavior in their work, using Si, Al-BEA and Si-MCM-41 [33]. When they carried out
340 their reaction over as-synthesized Si, Al-BEA catalyst, they had to use three times the amount
341 of the catalyst than that used for siliceous Si-MCM-41 to achieve comparable conversions.

342 From the three tested catalysts, Si-MCM-41 mesoporous silica showed to have the highest
343 catalytic activity in the cycloaddition reaction. This result is well correlated to the physico-
344 chemical characterizations of these materials (DRX, EDX, N_2 sorption) and also to their range
345 of features: (1) they are siliceous materials containing a high number of siloxy anion,

346 (2) capacity of the large pores to hold higher amounts of surfactant, which are cationic CTA⁺
347 in concert with siloxy anions [58], (3) CTA⁺ cations are bulky organic cations (low
348 charge/volume ratio) and this means that their interaction with the catalytic active sites, i.e.
349 siloxy anions, is weaker.

350 We have demonstrated using TGA analysis that removal of the surfactant (CTA⁺) in the
351 Si-MCM-41 is easier compared to Ga or Al-MCM-41, which means that the interaction
352 between the silica matrix and CTA⁺ is low whereas in the case of Ga or Al-MCM-41 the
353 interaction between the heteroatom-containing matrix and CTA⁺ is important. EDX analysis
354 also shows that the incorporation of aluminum is more important compared to the gallium
355 thus the Ga-MCM-41 has a high number of siloxy compared to Al-MCM-41 (see table 1).

356 Otherwise, triethylamine is at the origin of the irreversible water elimination step [50].
357 The latter may displace the reaction towards the formation of the final triazole, and thus help
358 to perform more difficult reactions such as that giving **3e** (absence of intramolecular hydrogen
359 bond to favor the enimine form).

360 Using triethylamine alone leads to an efficient reaction, except from α -
361 benzoylacetophenone (**2d**) and malonodinitrile (**2e**). Whereas for the former steric hindrance
362 can be proposed to rationalize the low yield, the absence of intramolecular hydrogen bond to
363 favor the enimine form can be advanced for the latter.

364 Using triethylamine in the presence of 10% of MCM-41 allowed the yields of **3d** and **3e**
365 to be improved. In the case of **3d**, calcined Si-MCM-41, which possesses a larger surface
366 area, proved the most efficient catalyst. The presence of surfactant inside the mesopores, by
367 decreasing the available surface, reduces the catalyst activity. In the case of **3e**, the yield is
368 increased whatever the catalyst employed. The latter can either favor the formation of the
369 enimine form or the 1,3-dipolar cycloaddition through coordination of the dipolarophile
370 nitrogen to the catalyst metal.

371 Without triethylamine, using as-synthesized MCM-41 catalysts in a sufficient amount (25
372 mol%) provides the triazoles **3a-c** (for which the enol forms are favored due to
373 intramolecular hydrogen bond) in good yields. In this case, the triethylamine effect can be
374 restored by the siloxy anions contained in as-synthesized MCM-41 catalysts. Substrate and
375 intermediate product size seems to be a limit of the system (products **3d** and **3e**), with better
376 yields noted for Si-MCM-41.

377 If we compare our materials with others catalysts, the as-synthesized Si-MCM-41 catalyst
378 seems to be the best for the reactions of cycloaddition [29,45]. In fact, not only the reaction
379 time is decreased (around 15 min) , but also the Si-MCM-41 is used as synthesized thus no
380 further preparation is needed.

381

382 - *Catalyst reusability*

383 Reusability of the catalysts has been studied in the cycloaddition of 4-nitrophenyl azide
384 (**1**) under the following conditions: 4-nitrophenyl azide (**1**, 1 mmol), acetylactone (**2a**, 1
385 mmol), as-synthesized Si- Ga- or Al-MCM-41 (25 mol%), DMF (2 ml), room temperature,
386 0.25h reaction time for Si-MCM-41, 1h for Ga-MCM-41 and 24 h for Al-MCM-41. The
387 catalysts were filtered, washed with DMF and dried before use in the following cycles, the
388 results are represented in the figure 6.

389 The catalyst could be reused up to five times with little loss of activity, confirming its
390 stability as seen by TGA and XRD data (fig.3S and fig.4S see supplementary data).

391 Indeed, the results obtained by the TGA analysis (fig.3S see supplementary data) indicate that
392 there is a weak CTA⁺ leaching from the reaction medium (for example ca. 0.2%, after five
393 use of as-synthesized Si-MCM-41). This mass loss is probably responsible for the slight
394 reduction of the catalyst activity. Concerning the results obtained by XRD analysis (fig.4S see
395 supplementary data) we note that there was a small decrease in the intensity of all

396 characteristic peaks of MCM-41, may be due to the influence of the solvent on the CTA
397 containing mesoporous materials [56].

398

399 **4. Conclusion**

400 Si- Ga or Al-MCM-41 molecular sieves have been successfully prepared by a direct
401 synthesis method. The samples exhibited high structural regularity and surface area values,
402 EDX results showed a more important incorporation of aluminum into the framework of
403 MCM-41 compared to gallium.

404 Three types of catalysts were compared in the course of the thermal cycloaddition of aryl
405 azides with activated alkenes, i.e. homogeneous [50], heterogeneous and mixed
406 homogeneous/heterogeneous catalysts. Concerning the latter two catalysts, the reaction time
407 and product yields of **3a-c** have been improved in the following order: heterogeneous catalyst
408 > mixed catalyst > homogeneous catalyst and, for the products **3d** and **3e**, the
409 homogeneous/heterogeneous catalysis was superior than the catalysts used individually. This
410 later result may be explained by a synergic effect between Et₃N and the mesoporous material.

411 The as-synthesized Si-MCM-41 is particularly efficient for the cycloaddition reaction at
412 room temperature due to its higher number of ionic pairs $\equiv\text{SiO}^- \text{CTA}^+$.

413 The incorporation of moderate amount of heteroatoms such as Al or Ga in the silica
414 framework would allow the mesoporous solids to benefit from enhanced hydrothermal
415 stability a feature particularly needed in reactions operating in aqueous media. Unfortunately,
416 heteroatom incorporation reduces the number of siloxy and decreases the basic character.

417 In conclusion, we have developed a convenient method for the synthesis of 1,2,3-triazoles,
418 which can serve as useful building blocks for useful targets, by Si-MCM-41-catalyzed
419 cycloaddition of aryl azides with activated alkenes in very high yields. This one-pot synthesis
420 of 1,2,3-triazoles using a heterogeneous catalytic system benefits from considerable synthetic

421 advantages, such as mild reaction conditions, easy availability of starting materials, short
422 durations of reaction (15 min), simplicity of the reaction procedure, efficient catalyst
423 regeneration and reuse for new reaction cycle.

424

425 **REFERENCES:**

426 [1] M.E. Davis, *Nature* 417 (2002) 813–821.

427 [2] I. Izquierdo-Barba, S. Sánchez-Salcedo, M. Colilla, M.J. Feito, C. Ramírez-Santillán,
428 M.T. Portolés, M. Vallet-Regí, *Acta Biomaterialia* 7 (2011) 2977–2985.

429 [3] P. Selvam, S.K. Bhatia, C.G. Sonwane, *Ind. Eng. Chem. Res.* 40 (2001) 3237–3261.

430 [4] S. Haddoum, I. Fechete, B. Donnio, F. Garin, D. Lutic, C.E. Chitour. *Catal. Comm.* 27
431 (2012) 141–147.

432 [5] J.J. Zou, Y. Liu, L. Pan, L. Wang, X. Zhang. *Appl. Catal. B: Environmental* 95 (2010)
433 439–445.

434 [6] J. Lin, B. Zhao, Y. Cao, H. Xu, S. Ma, M. Guo, D. Qiao, Y. Cao. *Appl. Catal. A: General*
435 478 (2014) 175–185.

436 [7] I. Fechete, B. Donnio, O. Ersen, T. Dintzer, A. Djeddi, F. Garin. *Appl. Surf. Sci.* 257
437 (2011) 2791–2800.

438 [8] B. Boukoussa, R. Hamacha, A. Morsli, A. Bengueddach, *Arab. J. Chem.* (2013),
439 <http://dx.doi.org/10.1016/j.arabjc.2013.07.049>.

440 [9] J. M. Campos, J. P. Lourenço, A. Fernandes, M. Rosário Ribeiro. *Catal. Comm.* 10 (2008)
441 71–73.

442 [10] A. Benhamou, J.P. Basly, M. Baudu, Z. Derriche, R. Hamacha, *J. Colloid Interface Sci.*
443 404 (2013) 135–139.

444 [11] S.A. Idris, S.R. Harvey, L.T. Gibson, *J. Hazard. Mater.* 193 (2011) 171–176.

445 [12] S. Yan, L. Xiu-Wu, S. Wei, Z. Yaping, Z. Li, *Appl. Surf. Sci.* 253 (2007) 5650–5655.

- 446 [13] G. Maria, A.I. Stoica, I. Luta, D. Stirbet, G. L. Radu, *Micro. Meso. Mater.* 162 (2012)
447 80–90.
- 448 [14] H. Yu, H. Zhang, W. Yang, J. Feng, W. Fan, S. Song, *Micro. Meso. Mater.* 170 (2013)
449 113–122.
- 450 [15] X. Liu, H. Sun, Y. Yang, *J. Colloid Interface Sci.* 319 (2008) 377–380.
- 451 [16] P.R. Selvakannan, K. Mantri, J. Tardio, S.K. Bhargava, *J. Colloid Interface Sci.* 394
452 (2013) 475–484.
- 453 [17] B.P. Ajayi, B. Rabindran Jermy, K.E. Ogunronbi, B.A. Abussaud, S. Al-Khattaf, *Catal.*
454 *Today* 204 (2013) 189–196.
- 455 [18] E. Martínez-Belmonte, J. Aguilar, M. Gutierrez, J.A. Montoya, J.A. De los Reyes, M.
456 Torres, L.F. Chen, *Catal. Today* 212 (2013) 45–51.
- 457 [19] N. Saadatjoo, M. Golshekan, S. Shariati, H. Kefayati, P. Azizi, *J. Mol. Catal. A: Chem.*
458 377 (2013) 173–179.
- 459 [20] B. Qi, Y. Wang, L.L. Lou, L. Huang, Y. Yang, S. Liu, *J. Mol. Catal. A: Chem.* 370
460 (2013) 95–103.
- 461 [21] E. Rezaei, J. Soltan, *Chem. Eng. J.* 198–199 (2012) 482–490.
- 462 [22] D. Zhang, R. Wang, L. Wang, X. Yang, *J. Mol. Catal. A: Chem.* 366 (2013) 179–185.
- 463 [23] E.G. Vaschetto, G.A. Monti, E.R. Herrero, S.G. Casuscelli, G.A. Eimer, *Appl. Catal. A:*
464 *Gen.* 453 (2013) 391–402.
- 465 [24] C.N. Pérez, E. Moreno, C.A. Henriques, S. Valange, Z. Gabelica, J.L.F. Monteiro,
466 *Micro. Meso. Mater.* 41 (2000) 137.
- 467 [25] S. Ernst, T. Bongers, C. Casel, S. Munsch, in: I. Kiricsi, G. Pál-Borbély, J.B. Nagy, H.G.
468 Karge (Eds.), *Porous Materials in Environmentally Friendly Processes, Studies in Surface*
469 *Science and Catalysis*, vol. 125, Elsevier, Amsterdam, 1999, p. 367.

- 470 [26] K.R. Kloetstra, M. van Laren, H. van Bekkum, *J. Chem. Soc., Faraday Trans.* 93 (1997)
471 1211.
- 472 [27] C.-M. Yang, K.-J. Chao, *J. Chin. Chem. Soc.* 49 (2002) 883.
- 473 [28] F. Fajula, D. Brunel, *Micro. Meso. Mater.* 48 (2001) 119.
- 474 [29] S. Roy, T. Chatterjee, M. Pramanik, A. S. Ro, A. Bhaumik, Sk. Manirul Islam. *J. of*
475 *Molec. Catal. A: Chemical* 386 (2014) 78–85.
- 476 [30] X. Wang, Y.-H. Tseng, J. C.C. Chan, S. Cheng, *J. Catal.* 233 (2005) 266.
- 477 [31] L. Martins, W. Hölderich, P. Hammer, D. Cardoso, *J. Catal.* 271 (2010) 220–227.
- 478 [32] Y. Kubota, H. Ikeya, Y. Sugi, T. Yamada, T. Tatsumi, *J. Mol. Catal. A: Chem.* 249
479 (2006) 181–190.
- 480 [33] R. Srivastava, D. Srinivas, P. Ratnasamy, *Tetrahedron Lett.* 47 (2006) 4213–4217.
- 481 [34] Y. Kubota, Y. Nishizaki, H. Ikeya, M. Saeki, T. Hida, S. Kawazu, M. Yoshida, H. Fujii,
482 Y. Sugi, *Micro. Meso. Mater.* 70 (2004) 135.
- 483 [35] A.C. Oliveira, L. Martins, D. Cardoso, *Micro. Meso. Mater.* 120 (2009) 206–213.
- 484 [36] A.R. Katritzky, Z. Yuming, S.K. Singh, *Heterocycles* 60 (2003) 1225–1239.
- 485 [37] M.J. Genin, D.A. Allwine, D.J. Anderson, M.R. Barbachyn, D.E. Emmert, S.A. Garmon,
486 D.R. Graber, K.C. Grega, J.B. Hester, D.K. Hutchinson, J. Morris, R.D. Reischer, D. Stper,
487 B.H. Yagi, *J. Med. Chem.* 43 (2000), 953–970.
- 488 [38] H. Wamhoff, in *Comprehensive Heterocyclic Chemistry*, ed. by A.R. Katritzky, C.W.
489 Rees (Pergamon, Oxford, 1984), pp. 669–732.
- 490 [39] D.R. Buckle, C.J.M. Rockell, H. Smith, B.A. Spicer. *J. Med. Chem.* 29 (1986) 2262–
491 2267.
- 492 [40] J.L. Kelley, C.S. Koble, R.G. Davis, E.W. Mclean, F.E. Sorako, B.R. Cooper, *J. Med.*
493 *Chem.* 38 (1995) 4131–4134.

- 494 [41] R.G. Mecetich, S.N. Maiti, P. Spevak, T.W. Hall, S. Yamabe, N. Ishida, M. Tanaka, T.
495 Yamazaki, A. Nakai, K. Ogawa, *J. Med. Chem.* 30 (1987) 1469–1474.
- 496 [42] R. Alvarez, S. Velazquez, A. San-Felix, S. Aquaro, E. De Clercq, C.F. Perno, A.
497 Karlsson, J. Balzarini, M.J. Camarasa. *J. Med. Chem.* 37 (1994), 4185–4194.
- 498 [43] R. Huisgen, *Angew. Chem.* 75 (1963) 604–637.
- 499 [44] V.V. Rostovtsev, L.G. Green, V.V. Fokin, K.B. Sharpless, *Angew. Chem. Int. Ed.* 41
500 (2002) 2596–2599.
- 501 [45] I. Jlalía, F. Gallier, N. Brodie-Linder, J. Uziel, J. Augé, N. Lubin-Germain, *J. Molec.*
502 *Catal. A: Chemical* 393 (2014) 56–61.
- 503 [46] S. Chassaing, M. Kumarraja, A. Sani Souna Sido, P. Pale, J. Sommer, *Org. Lett.* 9 (2007)
504 883–886.
- 505 [47] B.H. Lipshutz, B.R. Taft, *Angew. Chem. Int. Ed.* 45 (2006) 8235–8238.
- 506 [48] S. Brunauer, P.H. Emmett, E. Teller, *J. Am. Chem. Soc.* 60 (1938) 309–319.
- 507 [49] E.P. Barrett, L.G. Joyner, P.H. Halenda, *J. Am. Chem. Soc.* 73 (1951) 373–380.
- 508 [50] S. Zeghada, G. Bentabed-Ababsa, A. Derdour, S. Abdelmounim, L.R. Domingo, J.A.
509 Saez, T. Roisnel, E. Nassar, F. Mongin, *Org. Biomol. Chem.* 9 (2011) 4295–4305.
- 510 [51] T.R. Pauly, Y. Liu, T.J. Pinnavaia, S.J.L. Billinge, T.P. Rieker, *J. Am. Chem. Soc.* 121
511 (1999) 8835–8842.
- 512 [52] C-F.Cheng, H.He, W.Zhou, J. Klinowski, J.A.S.Goncalves, L.F. Gladden, *J. Phys.*
513 *Chem.*, 100(1996)390.
- 514 [53] K.Okumura, K. Nishigaki, M. Niwa, *Micro. Meso. Mater.*, 44-45 (2001), 509-516.
- 515 [54] B. Jarry, F. Launay, J.P. Nogier, V. Montouillout, L. Gengembre, J.L. Bonardet, *Appl.*
516 *Catal. A.* 309 (2006) 177–186.
- 517 [55] H.Y. Lin, Y.L. Pan, Y.W. Chen, *J. Porous Mater.* 12 (2005) 151–164.
- 518 [56] X. Yang, Q. Guan, W. Li, *J. Env. Mana.* 92 (2011) 2939-2943.

519 [57] Z. El Berrichi, L. Cherif, O. Orsen, J. Fraissard, J.-P Tessonnier, E. Vanhaecke, B. Louis,
520 M.-J. Ledoux, C. Pham-Huu, *Appl. Catal. A: General* 298 (2006) 194–202

521 [58] L. Martins, T.J. Bonagamba, E.R. Azevedo, P. Bargiela, D. Cardoso, *Appl. Catal. A:*
522 *Gen.* 312 (2006) 77–85.

523 [59] N. Baccile, G. Laurent, C. Bonhomme, P. Innocenzi, F. Babonneau, *Chem. Mater.* 19
524 (2007) 1343–1354.

525 [60] H. Koller, R.F. Lobo, S.L. Burkett, M.E. Davis, *J. Phys. Chem.* 99 (1995) 12588.

526

527

528

529

530 **Figure caption**

531 **Fig.1.** XRD patterns of as-synthesized and calcined Si- Ga- or Al-MCM-41, (a): Ga-MCM-41
532 and (b): Al-MCM-41. (c) Si-MCM-41

533 **Fig.2.** Nitrogen adsorption-desorption isotherms of calcined Si- Ga- or Al-MCM-41 materials.

534 **Fig.3.** TGA analysis curves for as-synthesized Si- Ga- or Al-MCM-41 mesoporous materials
535 photomicrographs of calcined (a) Ga-MCM-41 and (b) Al-MCM-41.

536 **Fig.4.** SEM and TEM images of calcined Si- Ga- or Al-MCM-41 mesoporous materials:
537 (a,b,c) SEM images, (d,e,f) TEM images.

538 **Fig.5.** Effect of the catalyst amount (as-synthesized Ga-MCM-41) on the yield of **3a**.

539 **Fig.6.** Catalyst reusability. Reaction conditions: 4-nitrophenyl azide (**1**, 1 mmol),
540 acetylacetone (**2a**, 1 mmol), catalyst (25 mol %), DMF (2 mL), room temperature,
541 reaction time: 0.25h (15min) for Si-MCM-41, 1h for Ga-MCM-41 and 24h for Al-
542 MCM-41 (at the end of the reaction, the catalyst is dried and reused).

543

543 **Table 1.** Physical characteristics of mesoporous catalysts.

Catalyst (calcined)	Si/M ^a	Si/M (EDX) ^b	d_{100} (Å)	a_0 (Å) ^c	Surface area (m ² /g)	D^d (Å)	h^e (Å)	Pore volume (cm ³ /g)
Si-MCM-41	//	//	37.54	43.34	1430	35.2	8.14	1.071
Al-MCM-41	80	90.74	41.24	47,61	1440	35.7	11.91	1.097
Ga-MCM-41	80	100.01	42.42	48,98	1030	36.7	12.28	0.973

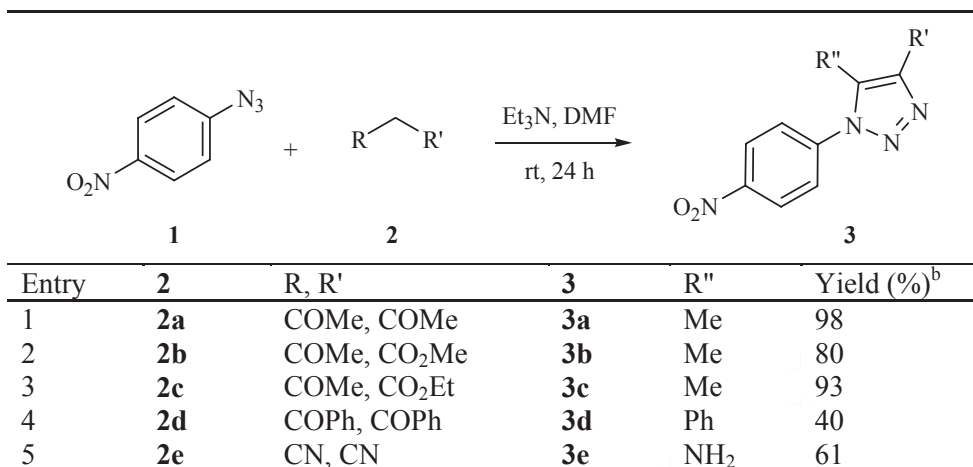
544

545 ^a Molar ratio in the initial gel. M = Ga or Al546 ^b Molar ratio determined by EDX analysis547 ^c a_0 means lattice parameter: $a_0 = 2d_{100}/\sqrt{3}$ 548 ^d Pore diameter determined by the BJH method549 ^e h : wall thickness: $h = a_0 - D$

550

550

551 **Table 2.** Cycloaddition reaction of 4-nitrophenyl azide (**1**) with the activated alkenes **2**
 552 performed at room temperature.



553

554 ^a Reaction conditions: 4-nitrophenyl azide (**1**, 1 mmol), activated alkene (**2**, 2 mmol), Et₃N (2
 555 mmol), DMF (2 mL), room temperature, 24 h (see procedure 1).

556 ^b Isolated yields.

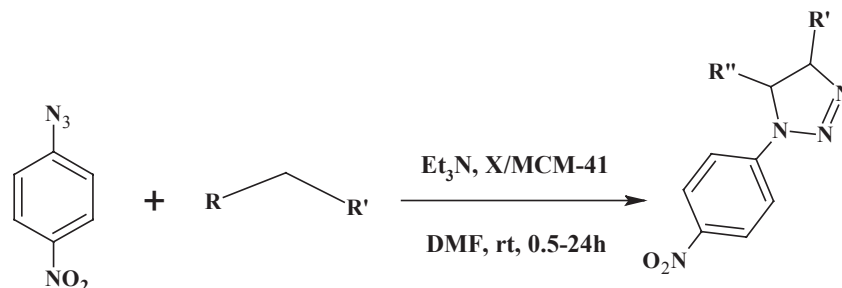
557

557

558

559

560

Table 3. Cycloaddition reaction of 4-nitrophenyl azide (**1**) with the activated alkenes **2** catalyzed under homogeneous/heterogeneous catalysis^a.

X: calined ou as-synthesized

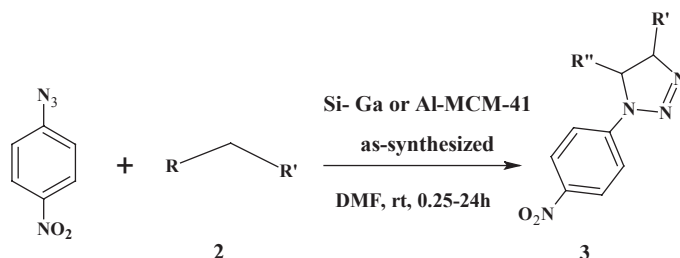
Entry	2	Catalyst	3	T (h)	Yield (%) ^b
1	2a	calcined Ga-MCM-41	3a	1.5	97
2	2b		3b	1.5	94
3	2c		3c	1.5	51
4	2d		3d	24	53
5	2e		3e	2	71
6	2a	as-synthesized Ga-MCM-41	3a	1.5	90
7	2b		3b	1.5	98
8	2c		3c	1.5	54
9	2d		3d	24	47
10	2e		3e	2	97
11	2a	calcined Al-MCM-41	3a	1.5	98
12	2b		3b	1.5	91
13	2c		3c	1.5	95
14	2d		3d	24	84
15	2e		3e	2	88
16	2a	as-synthesized Al-MCM-41	3a	1.5	98
17	2b		3b	1.5	97
18	2c		3c	1.5	55
19	2d		3d	24	59
20	2e		3e	2	78
21	2a	calcined Si-MCM-41	3a	0.5	98
22	2b		3b	0.5	93
23	2c		3c	0.5	95
24	2d		3d	24	88
25	2e		3e	0.5	92
26	2a	as-synthesized Si-MCM-41	3a	0.5	98
27	2b		3b	0.5	90
28	2c		3c	0.5	97
29	2d		3d	24	79
30	2e		3e	0.5	98

561

562 ^a Reaction conditions: 4-nitrophenyl azide (**1**, 1 mmol), activated alkene (**2**, 2 mmol), Et₃N
 563 (homogeneous catalyst, 2 mmol), heterogeneous catalyst (10 mol%), DMF (2 mL), room
 564 temperature (see procedure 2), 0.5-24 h.

565 ^b Isolated yields.

566 **Table 4.** Cycloaddition reaction of 4-nitrophenyl azide (**1**) with the activated alkenes **2**
 567 catalyzed by as-synthesized Si- Ga- or Al-MCM-41^a.



Entry	2	Catalyst	3	T (h)	Yield (%) ^b
1	2a	as-synthesized Ga-MCM-41	3a	1	92
2	2b		3b	1	93
3	2c		3c	1	94
4	2d		3d	24	47
5	2e		3e	24	9
6	2a	as-synthesized Al-MCM-41	3a	24	89
7	2b		3b	24	61
8	2c		3c	24	71
9	2d		3d	24	48
10	2e		3e	24	8
11	2a	as-synthesized Si-MCM-41	3a	0.25	94
12	2b		3b	0.25	97
13	2c		3c	0.25	90
14	2d		3d	24	69
15	2e		3e	18	55

568

569 ^a Reaction conditions: 4-nitrophenyl azide **1** (1 mmol), activated alkene **2** (1 mmol), as-
 570 synthesized Si- Ga- or Al-MCM-41 (25 mol%), DMF (2 mL), room temperature (see
 571 procedure 3), reaction time 0.25-24h

572 ^b Isolated yields.

573

574

575

576

Figure

Fig 1

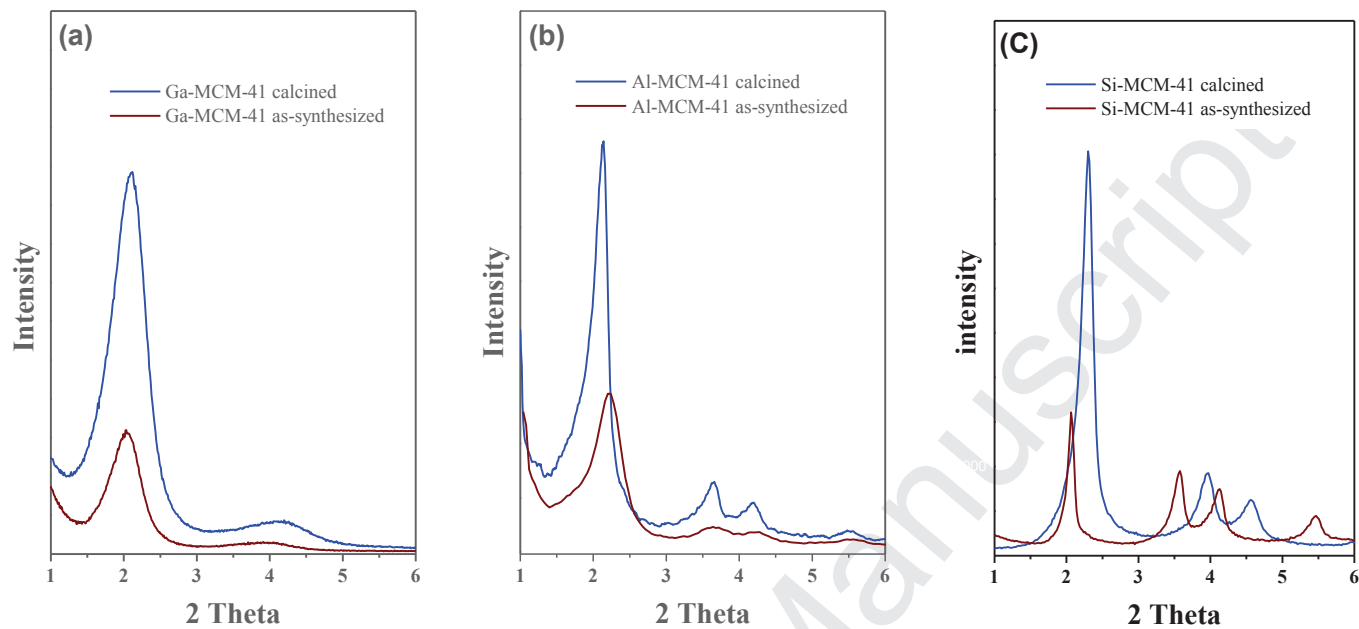


Fig 2

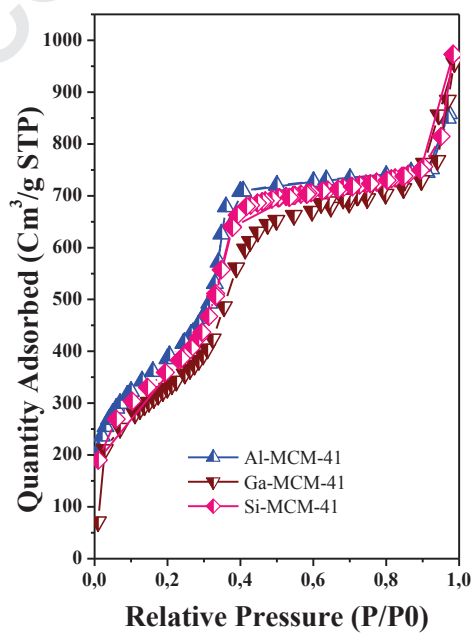


Fig 3

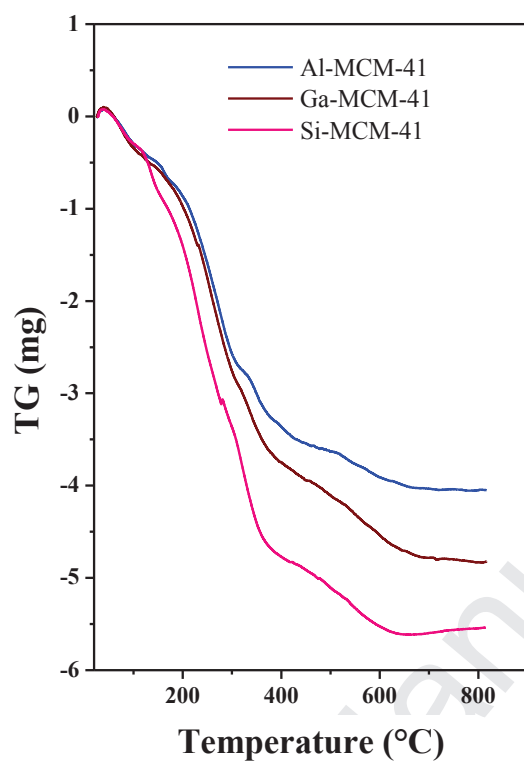


Fig 4

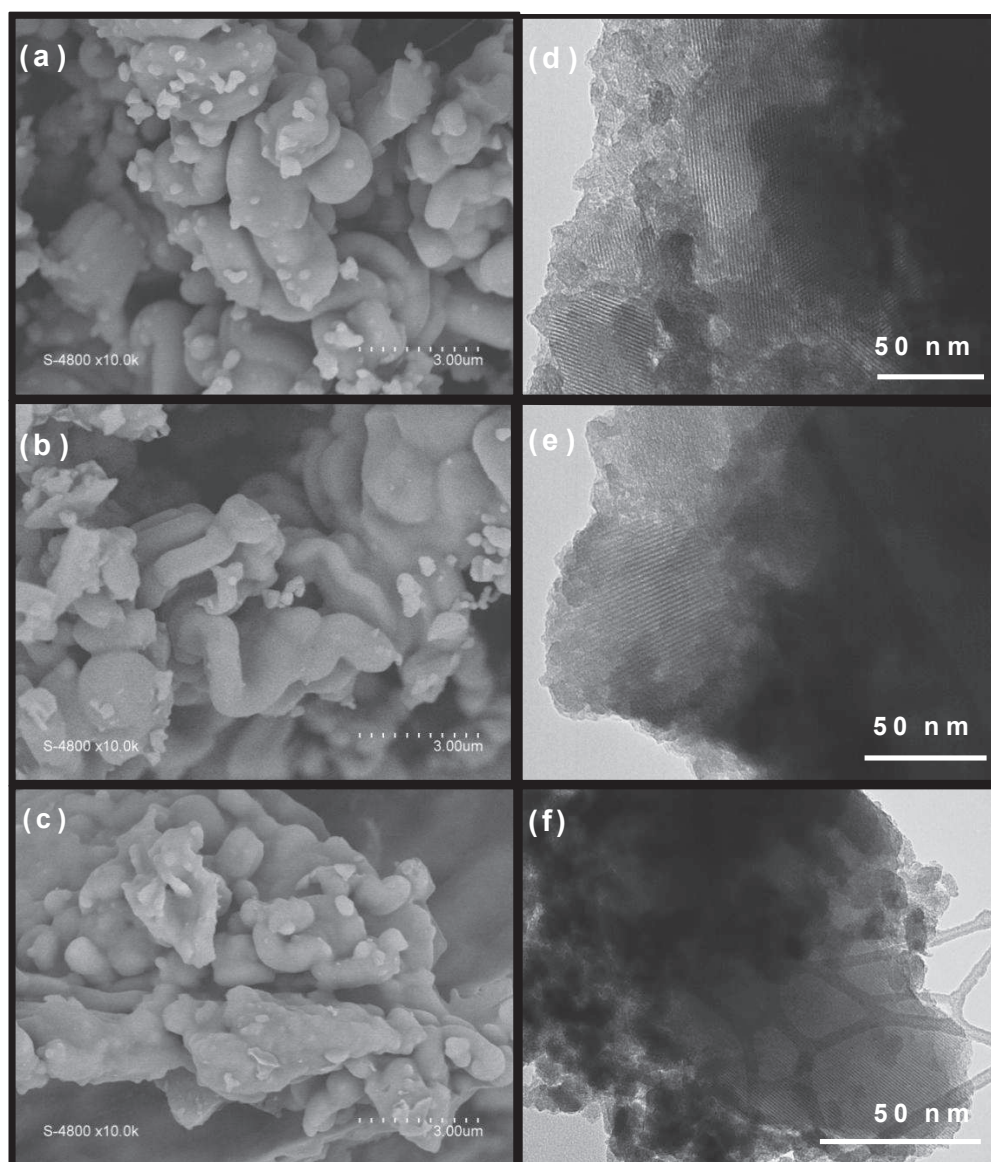


Fig 5

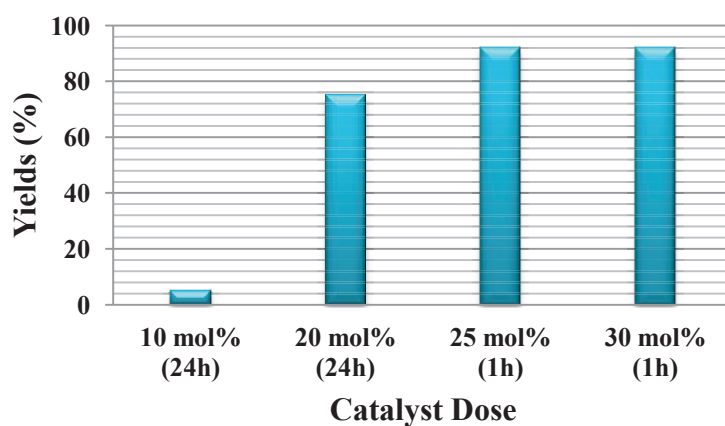


Fig 6

